Heteroatom Chemistry
Volume 17, Number 6, 2006

# Quantitative Analysis of Bonding in $P_4$ Clusters

V. G. Tsirelson, N. P. Tarasova, M. F. Bobrov, and
Yu. V. Smetannikov

*D. I. Mendeleyev University of Chemical Technology of Russia, Miusskaya sq., 9,
Moscow 125047, Russia*

*Received 9 December 2005; revised 21 April 2006*

ABSTRACT: *Quantum-topological analysis based on the nonempirical quantum-chemical calculations of $P_4$ clusters in the different electronic states has been done. Changes in the geometric parameters for the different electronic states of the equilibrium phosphorus clusters and structures with the breaking bonds are traced. The P—P bonds are quantitatively described.* DOI 10.1002/hc.20279

## *INTRODUCTION*

The properties of allotropic modifications of elemental phosphorus [1,2] capable of the transmutations [3] are determined by their electronic structure. Depending on the reaction conditions, white phosphorus is capable of manifesting both nucleophilic and electrophilic properties, which determine the variety of products including the polymeric systems [4–7]. The construction of a polymer assumes the participation in the process of the reactive intermediate particles derived from tetraphosphorus. One of the examples of reactions in which the appearance of $P_4$ clusters of different structures is expected is a bulk polymerization of the white phosphorus producing the red modification. It is known that industrial scale production of red phosphorus leads to an end product with poorly reproducible physicochemical properties [8] mainly due to the specific conditions of the polymer synthesis [3]. It is obvious that reaction conditions in the extreme case determine the probability of breaking one of the P—P bonds in the $P_4$ cage molecule with the retention of the tetraatomic group. In this case, the formation of the red phosphorus polymers of both linear and three-dimensional structure is possible. Experimental data [9] and Monte Carlo simulations [10] have shown that the $P_4$ liquid phase, while being stable at low pressure, $P$, and relatively low temperature, $T$, transforms to a polymeric state by increasing either $P$ or $T$. These phase changes were observed in recent experiments with similar thermodynamic conditions, as shown by a close agreement of computed and measured structure factors in the molecular and polymer phases [10].

From the point of view of the initial transformation of tetraphosphorus into the red modification, the polymerization can be viewed as consisting of the following stages: the formation of the reactive intermediates on the basis of tetraphosphorus, the formation of $P_n$-clusters, and the formation of the three-dimensional polymer. There are evidences confirming the existence of the last two stages [11], whereas the information about the nature and structure of the particles initiating the polymerization is very limited. In particular, it is known that during

---

*Correspondence to:* N. P. Tarasova; e-mail: tarasnp@muctr.edu.ru.

the X-ray irradiation of the $P_4$ solution in $CFCl_3$ at 77 K, the formation of the cation-radical $P_4^+$ [12] with the degenerate Jahn–Teller unstable triplet electronic state $^2E$ [12] occurs. As a result, one of the bonds in the initial tetrahedral structure breaks and the so-called "butterfly"-structure with $D_{2d}$ symmetry is formed. The mechanism of this transformation agrees with the ESR results [12]. X-ray diffraction analysis of the complex $((Fe(CO)_4(\mu\text{-}P_2))_2(\mu\text{-}Fe_2(CO)_6)_2$, formed in the reaction of white phosphorus with $Fe_2(CO)_9$ in boiling benzene, has confirmed the existence of the planar $P_4$ fragment [13]. There is also some evidence of the formation of the tetraphosphorus anion [14]. Other data [15] attest that the $P_4$ fragment has cage, plane, zigzag, and other intermediate configurations.

In the synthesis of phosphorus-based polymers, the variation of the reaction conditions shows the specific mechanisms of its formation—radical, ionic, or mixed. Unfortunately, the absence of the uniform detailed analysis of electronic properties of the neutral and ionic phosphorus clusters does not allow us to judge from the experimental results of white phosphorus polymerization [16]. Meanwhile, one might suggest that various allotropic modifications of the elemental phosphorus are caused by its unique electronic system. However, their experimental study is rather complicated due to the high reactivity of such systems. Thus, the quantum-chemical analysis of bonding in the phosphorus clusters is especially important. Moreover, the study of the local electronic properties of the P—P bonds makes it possible to quantify the atomic interactions in $P_4$ clusters.

Calculations of $P_n$ clusters ($n = 2$–89) have been carried out and the geometry and relative stability of the isomers evaluated [15,17–19]. However, the detailed picture of the chemical bond in the phosphorus clusters has not been examined until now. Initially, the description of $P_4$ electronic structure was limited to the hybrid orbital scheme [20,21]. Later, the analysis of the electron density maps derived by nonempirical calculations has made it possible to attain the semiquantitative correspondence of the calculated and experimental electron absorption spectra [18]. It was also found that the maxima of the valence electron concentrations on the bond lines in $P_4$ are shifted from the internuclear vectors outside the center of molecule—a typical picture for bent bonds. It was also assumed that the presence of $\pi$-bonds influences the structure of a $P_4$ molecule [18]. At the same time, the assumption about the possible linear structure of the polymer consisting of open $P_4$ fragments [20] was not confirmed [15].

More recently nonempirical quantum-chemical calculations [15,22] showed that in the general $P_n$ structure ($n = 5, 6, 7, 8, \ldots$), it is possible to identify clusters consisting of distorted $P_4$ tetrahedra. This fact determines the importance of the comprehensive chemical bond analysis of $P_4$ clusters.

In this work, we have used for the first time the topological analysis of electron density (ED) [23–25] to analyze the bonding in the neutral $P_4$ cluster, as well as in the positive $P_4^+$ and negative $P_4^-$ ions, respectively. The structure of the nonequilibrium $P_4$ fragments has been studied as well. We have also considered the reaction ability of these compounds.

The topological analysis of ED is the part of the Bader topological theory of the molecular structure [23–25], which makes it possible to analyze the structure of molecules and the nature of the chemical bond. It deals with characteristics of the ED, calculated nonempirically or derived experimentally from X-ray diffraction data [25]. The features of the molecular structure are characterized using the parameters of the critical points in electron density—the ones where the ED gradient is equal to zero. The bond critical point (BCP), which is placed on the ED "bridge" connecting the neighboring nuclei, the bond path, is most important for describing the atomic interactions. ED value at the BCP, $\rho_b$, characterizes the strength of the interatomic interactions and correlates well with the bond energy and the bond order [23]. The principal curvatures of the electron density at the BCP, $\lambda_1 < \lambda_2 < \lambda_3$, along three mutually perpendicular directions ($\lambda_3$ is the ED curvature along the bond path) as well as the Laplacian of the electron density, $\nabla^2\rho_b = \lambda_1 + \lambda_2 + \lambda_3$, characterize the spatial distribution of electrons. The bond ellipticity, $\varepsilon = |\lambda_1/\lambda_2| - 1$, gives the measure of the ED accumulation in the plane perpendicular to the bond path: $\varepsilon > 0$ is typical for the bonds having the $\pi$-component. The regions of electron concentration exhibit $\nabla^2\rho < 0$, while the regions of the electron depletion exhibit $\nabla^2\rho > 0$. Thus, Laplacian of electron density indicates the presence and arrangement of electron pairs [15]. In addition, the kinetic energy density, $g_b > 0$, and potential energy density, $v_b < 0$, as well as the total electronic energy $h_b = g_b + v_b$ at the BCP characterize the type of interatomic interaction. Shared atomic interactions (covalent bond) show $\rho_b > 0.15$, $|\lambda_1|/\lambda_3 > 1$, $\nabla^2\rho_b < 0$, $h_b < 0$ [15,26–28]. The closed-shell interactions (ionic, metallic, and van der Waals bonds) show $\rho_b < 0.07$, $|\lambda_1|/\lambda_3 < 0.25$, $\nabla^2\rho_b > 0$, $h_b > 0$. The intermediate interactions take place if $0.07 < \rho_b < 0.15$ a.u., $|\lambda_1|/\lambda_3 > 0.20$, $\nabla^2\rho_b > 0$, $h_b < 0$ [29,30]. The bond degree parameter $I_b = h(\mathbf{r_b})/\rho(\mathbf{r_b})$ [29] provides an additional quantification of atomic interactions: the stronger the shared interaction, the more negative is the $I_b$ value, the weaker is the closed-shell interaction, and the greater is the value $I_b > 0$.

The two-dimensional ED minimum is present in the ring molecules; the corresponding critical point is called the ring critical point. The cage molecules exhibit the local ED minimum, which corresponds to the cage critical point [23].

## *COMPUTATIONAL*

The quantum-chemical calculations of the phosphorus clusters were done with the nonempirical Hartree–Fock method in the 6-311G** basis set; the program package GAMESS [30,31] was used. After geometry optimization, the structures corresponding to the local minima on the potential energy surface were selected on the basis of the vibration frequency analysis. The ED maps and Laplacian distributions were computed using the modified software package AIMPAC [26] adapted for IBM PC [21,27]. During the search for the critical points, the fulfillment of the Poincare–Hopf–Morse rule $N - B + R - C = 1$ [23] was checked ($N$ is the number of nuclei in the molecule, and $B$, $R$, and $C$ are the number of bond, ring, and cage critical points, respectively).

We also investigated a series of nonequilibrium structures with the torsional angle between the P—P—P plane and the direction to the fourth P atom in the range from 50° to 180°.

The obtained geometrical and energy characteristics of clusters as well as the BCP local electronic properties are given in Table 1.

## *RESULTS AND DISCUSSION*

1. The neutral $P_4$ cluster in the singlet electronic state has a structure of a regular tetrahedron with the internuclear distance of 2.181 Å, which is close to the value of 2.22 Å obtained by the B3LYP/6-311G(d) method [15]. Figure 1a depicts the molecular graph of this cluster. The BCP characteristics are listed in Table 1, and Figs. 1b and 1c evidence that the P—P bond in this cluster is an ordinary covalent one.

   The angle between the vector linking the phosphorus nuclei and the direction to the BCP is ~5°, i.e., the bond path is weakly bent from the center of P4 tetrahedron. This situation, in principle, is typical for strain bonds, the angle quantitatively reflecting the strain degree. The low value of this angle in the neutral $P_4$ cluster demonstrates that the bond strain is insignificant. Thus, the previously assumed essential bend of this bond [17] has not been confirmed.

   The regions of the negative Laplacian of ED (Fig. 1c) are placed around the BCP positions. They also peak behind the P atoms indicating the position of the electron lone-pairs, which can serve as the centers of electrophilic attack.

2. The energy of the neutral $P_4$ cluster in the triplet state is 24.44 kcal/mol higher than the energy of the neutral singlet-state cluster. This molecule has a structure of the open tetrahedron of the $D_{2d}$ symmetry with the dihedral angle between the planes equal to 107.30° (Table 1 and Fig. 2). The number and arrangement of the critical points in this cluster differ from that in the singlet state

**TABLE 1** Energy Characteristics and the Local Properties of Electron Density at the Critical Points of the Bonds of Clusters $P_4$

| | *Cluster* | | | | | | | | | |
|---|---|---|---|---|---|---|---|---|---|---|
| *Parameter* | $P_4^0$, $1T_d$ | $P_4^0$, $3C_{2v}$ | | $P_4^+$, $2T_d$ | $P_4^+$, $2D_{2h}$ | | $P_4^-$, $2C_{2V}$ | | | |
| Total energy (a.u.) | −1362.9837 | −1362.9447 | | −1362.5505 | −1362.6743 | | −1362.9381 | | | |
| $r$ (Å) | 2.181 | 2.198 | 2.211 | 2.234 | 2.385 | 2.142 | 2.188 | 2.193 | 2.222 | 2.477 |
| $\rho_b$ | 0.115 | 0.116 | 0.107 | 0.106 | 0.078 | 0.127 | 0.113 | 0.113 | 0.108 | 0.063 |
| $\varepsilon$ | 0.030 | 0.182 | 0.082 | 0.162 | 0.330 | 0.043 | 0.051 | 0.049 | 0.098 | 0.479 |
| $\nabla^2\rho_b$ | −0.134 | −0.145 | −0.097 | −0.109 | 0.016 | −0.179 | −0.131 | −0.141 | −0.114 | 0.027 |
| $\lambda_1$ | −0.108 | −0.125 | −0.092 | −0.115 | −0.048 | −0.128 | −0.107 | −0.113 | −0.105 | −0.048 |
| $\lambda_2$ | −0.104 | −0.105 | −0.085 | −0.099 | −0.036 | −0.122 | −0.102 | −0.108 | −0.095 | −0.032 |
| $\lambda_3$ | 0.078 | 0.085 | 0.080 | 0.104 | 0.101 | 0.071 | 0.077 | 0.081 | 0.086 | 0.107 |
| $\lvert\lambda_1\rvert/\lambda_3$ | 1.385 | 1.471 | 1.150 | 1.106 | 0.475 | 1.803 | 1.390 | 1.395 | 1.221 | 0.449 |
| $v_b$ | −0.100 | −0.094 | −0.092 | −0.081 | −0.058 | −0.115 | −0.096 | −0.093 | −0.085 | −0.043 |
| $g_b$ | 0.033 | 0.029 | 0.034 | 0.027 | 0.031 | 0.035 | 0.032 | 0.029 | 0.028 | 0.025 |
| $h_b$ | −0.067 | −0.065 | −0.058 | −0.054 | −0.027 | −0.080 | −0.064 | −0.064 | −0.057 | −0.018 |
| $h_b/\rho_b$ | −0.583 | −0.560 | −0.542 | −0.509 | −0.346 | −0.630 | −0.566 | −0.566 | −0.528 | −0.286 |
| $g_b/\rho_b$ | 0.287 | 0.250 | 0.318 | 0.255 | 0.397 | 0.276 | 0.283 | 0.257 | 0.259 | 0.397 |

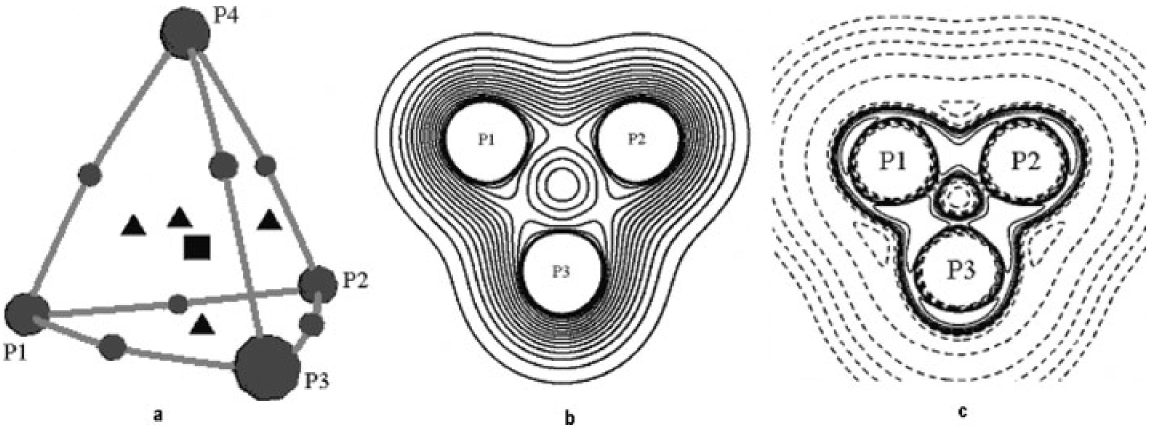

**FIGURE 1** The neutral cluster $P_4$ in the singlet state: (a) the molecular graph and the bond, ring, and cage critical points, which are shown as black circles, triangles, and squares, respectively; (b) electron density in the plane through three phosphorus atoms, line intervals are 0.05 a.u.; (c) Laplacian of the electron density in the same plane, the isolines are drawn at $\pm 2^n \times 10^m$ a.u. (where $n = 1, 2, 3$; $m = 0, \pm 1, \pm 2$). Solid lines correspond to $\nabla^2\rho \leq 0$; dashed lines denote the areas with $\nabla^2\rho > 0$.

(Table 1 and Fig. 2). BCP between the P1 and P2 atoms is arranged in the middle of the bond path, while the BCPs on the P1—P3 and P1—P4 bonds are displaced by 0.02 Å to the apical atom. The angle between the P1—P3 vector and the direction to the BCP is 3°, and this angle is ~4° for the P1—P3 and P1—P4 bonds. In other words, the bond paths are only weakly bent as it takes place in the neutral $P_4$ cluster in the singlet state.

The P1—P2 and P1—P3 bonds have different lengths although the topological characteristics given in Table 1 show that the type of the chemical bond between these atoms is the same. The P1—P2 distance is longer than the distances of P1—P3 and P1—P4—these bonds being longer than those in the neutral singlet-state cluster.

Electron density at the P1—P2 BCP is lower than that at the BCPs on the P1—P3 and P1—P4 bonds. The value $|\lambda_1|/\lambda_3$ is substantially smaller; however, for the P1—P3 and P1—P4 bond, $|\lambda_1|/\lambda_3$ is larger than those in the neutral singlet cluster. The absolute value of the electronic energy, $h_b$, and the bond degree parameter, $I_b$, are lower as well. Because the P1—P2 bond is weak, it determines the position of the reaction center when the reagent interacts.

In the open cluster, the atoms acquire the small net charge: its value is −0.04 *e* for P1 and P2 atoms and +0.04 *e* for P3 and P4 atoms. In addition, the centers of the electrophilic and nucleophilic attack appear in this cluster. The orbital bond orders of the P1—P2 and P1—P3 bonds in the triplet-state cluster are 0.96 and 0.91, respectively, somewhat lower than in the singlet state (0.97). The smaller bond order corresponds to the larger bond length. The ellipticity of the

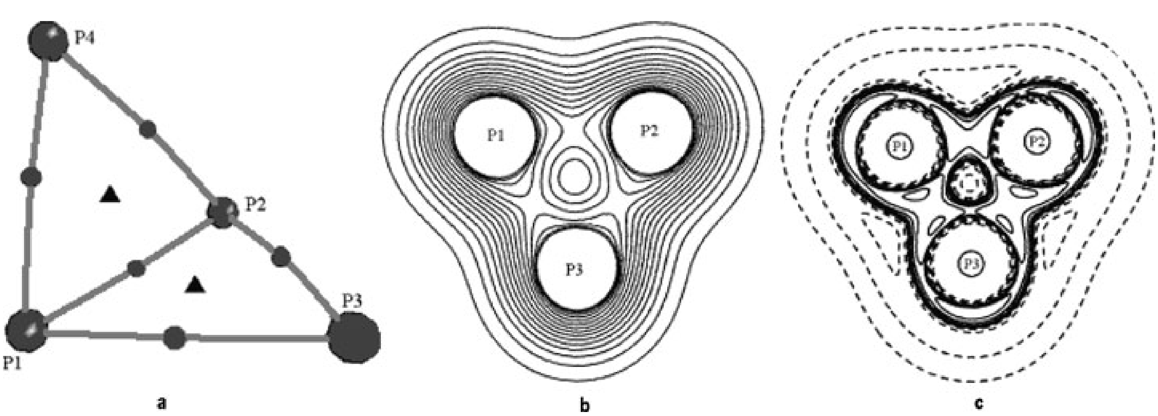

**FIGURE 2** The neutral cluster $P_4$ in the triplet state: (a) molecular graph and the critical points; (b) electron density; (c) Laplacian of the electron density. For more details, see legend to Fig. 1.

P1—P3 bond is insignificantly higher than that in the neutral P4 cluster, while the ellipticity of the P1—P2 bond is substantially higher. This indicates the nonequivalent contributions of the $\pi$-component to these bonds, and the electrons shift from the P3 and P4 atoms to the P1 and P2 atoms.

The ED value at the ring critical point in the P1—P2—P3 plane practically coincides with that in the singlet cluster. The positive Laplacian of electron density characterizing the charge depletion in this area is lower by 0.025 a.u.

3. The geometry optimization of the positive ion $P_4^+$ in the doublet electronic state with the regular tetrahedron starting geometry without imposing the symmetry restrictions yields a regular tetrahedron structure. The energy of this cluster is 271.83 kcal/mol higher than that of the neutral cluster, whereas the internuclear distances are 0.053 Å longer (Table 1 and Fig. 3). All the bonds in this cluster are equivalent; ED at the BCP is lower than in the neutral singlet-state cluster. The absolute values of the electronic energy, $h_b$, and the bond degree parameter, $I_b$, are smaller as well (Table 1). Thus, atoms in this cluster are weakly bonded and $P_4^+$ cluster is more reactive in comparison with the neutral singlet-state cluster.

   The geometry optimization of the $P_4^+$ cation with the starting geometry $D_{2h}$ (four "short" and two "long" bonds) led to the molecular structure of symmetry $D_{2h}$ (Fig. 4a). This result has been already reported in an earlier published paper [18]. The cation energy is 77.66 kcal/mol smaller than that of the regular tetrahedron-geometry cluster. The topological characteristics of the shared atomic interactions in this structure (Fig. 4c) differ from those in other clusters. The ED, electronic energy, and the bond degree parameter at the CPB show that the "short" bonds are stronger compared to the neutral singlet ones, while the "long" bonds are considerably weaker (Table 1). Nonequivalence of the bonds is distinctly manifested in the ED maps (Fig. 4b): in particular, they show that the electron concentration between the atoms P3 and P4 is smaller.

   Thus, positive ion $P_4^+$ in the doublet electronic state has two nuclear configurations; the more energy stable configuration has the $D_{2h}$ symmetry.

4. Geometry optimization of the negative ion, $P_4^-$, in the doublet electronic state with the starting geometry of a regular tetrahedron without imposing symmetry restrictions yielded a distorted $D_{2h}$ structure. Its energy 28.59 kcal/mol is higher than that of the neutral singlet cluster (Table 1 and Fig. 5). All the internuclear distances in the anion are longer that those in the neutral cluster. The cage critical point in this structure disappears; the ring critical point in the P2—P3—P4 plane disappears as well. The atomic charges are as follow: P1 −0.16 $e$, P2 and P3 −0.27 $e$, and P4 −0.31 $e$. Thus, the P4 atom is the most probable center of the electrophilic attack.

   The "longest" P—P bond of 2.477 Å exhibits the smallest $\rho_b$ and $|\lambda_1|/\lambda_3$ values as well as the smallest absolute values of the $h_b$ and $I_b$ parameters. This bond is the weakest among all the bonds in the $P_4$ clusters described in this work; it can be assumed that this cluster might be the most reactive.

   Recently, we have revealed the ionic channel of the radiation-induced polymerization of white phosphorus in dimethylsulfoxide [14]. Our computations show that the differences between the energy of the neutral singlet-state and neutral

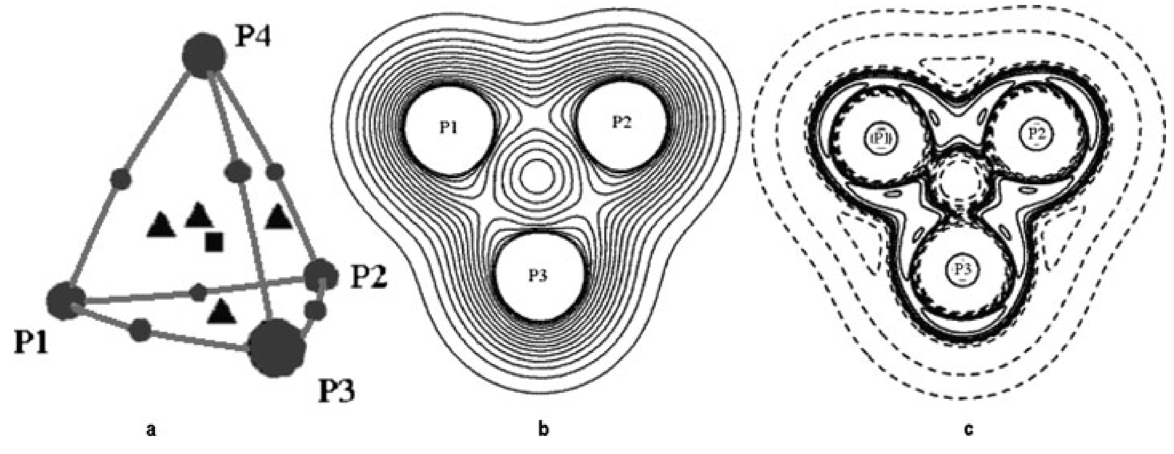

FIGURE 3 Positive ion $P_4^+$ with the $T_d$ symmetry in the doublet state: (a) molecular graph and the critical points; (b) electron density; (c) Laplacian of the electron density. For more details, see legend to Fig. 1.

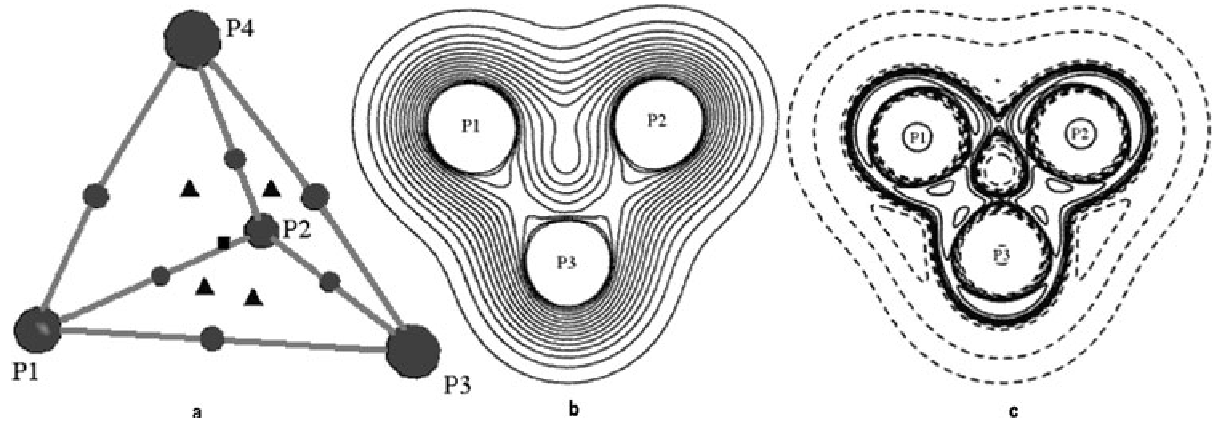

**FIGURE 4** Positive ion $P_4^+$ with $D_{2h}$ symmetry in the doublet state: (a) molecular graph and the critical points; (b) electron density; (c) Laplacian of the electron density. For more details, see legend to Fig. 1.

triplet-state $P_4$ clusters as well as the neutral singlet-state $P_4$ cluster and its anion are comparable. It increases the probability of the occurrence of the anionic polymerization channel. The participation of the $P_4^+$ cation in this reaction can be neglected.

5. To trace the energetics of the structure transformation of the $P_4$ phosphorus clusters, the calculations of different unstable conformations of the neutral $P_4$ cluster were carried out. The dihedral angle (DA) between the plane P1—P2—P3 and the direction to the P4 atom was changed step by step from 50° to 180° (in the equilibrium structure this DA is 70.528°). The DA decrease from the equilibrium value to 60° leads to 22.66 kcal/mol increase in the energy, whereas the increase in the DA to 80° increases energy only at 8.39 kcal/mol. The energy difference of 6.38 kcal/mol is observed at $110° < \text{TA} < 150°$; thus, the energy functional is flat and asymmetric. With the DA decrease to 50°, the P3—P4 distance decreases from equilibrium value of 2.181 Å to 1.596 Å, while the ED value of the P3—P4 bond increases. In both cases, a local ED maximum is observed between the atom pairs with the shorter internuclear distance. It is possible to say that the nonnuclear attractor arises during the approach of the atoms to each other instead of the BCP in the middle of the bond line in the neutral $P_4$. The two saddle points are formed between this attractor and adjacent P nuclei.

An increase in the DA angle from the equilibrium to 180° with an increase in the distance between the moved away P atoms from 2.181 Å to 3.777 Å diminishes the ED between them and increases the shift of electrons to the basins of

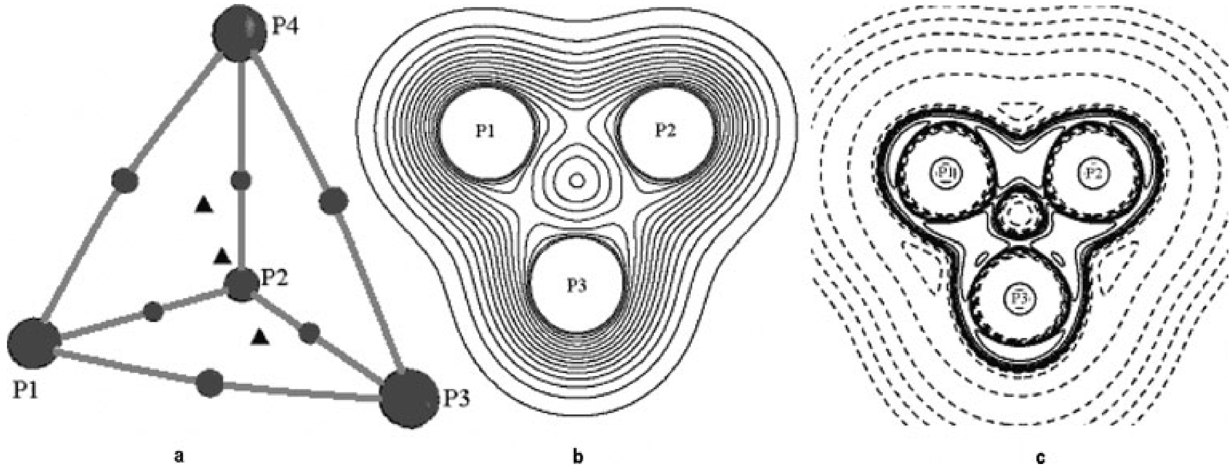

**FIGURE 5** Negative ion $P_4^-$ in the doublet state: (a) molecular graph and the critical points; (b) electron density; (c) Laplacian of the electron density. For more details, see legend to Fig. 1.

the P3 and P4 atoms. Beginning with TA > 90°, the local minimum inside the $P_4$ cluster is not revealed; simultaneously, one-dimensional minimum between the P3—P4 atoms disappears.

In conclusion, the geometrical parameters of the equilibrium $P_4$ clusters in different electronic states have been determined in this work using the nonempirical quantum-chemical calculations. The factors responsible for the chemical bond breaking under the temperature or X-ray irradiation have been discussed. It was found that the neutral $P_4$ cluster in the singlet electronic state has the lowest energy and is the most stable, while the $P_4^-$ cluster is probably the most reactive. This conclusion agrees with the fact that the rate of transformation in the radiation-induced polymerization of white phosphorus in the polar solvent is higher than that in the nonpolar solvent under the comparable conditions [14].

At the same time, relatively stable clusters capable of participating in the different transformations can be formed. The nonequivalence of the P atoms in all studied clusters, except the neutral $P_4$ cluster in the singlet electronic state, is accompanied by the redistribution of electron density, which leads to the formation of the positive and negative reactive centers.

## *REFERENCES*

[1] Corbridge, D. E. C. Phosphorus 2000. Chemistry, Biochemistry & Technology; Elsevier, Amsterdam, 2000; 1258 p.
[2] Simon, A.; Borrmann, H.; Horakh, J. Chem Ber 1997, 130(9) 1235–1240.
[3] Nad'yarnykh, G. V.; Tarasova, N. P. Chem Prom-st 1985, 11, 673–675.
[4] Tarasova, N. P.; Nad'yarnykh, G. V.; Kostikov, V. V.; Chistyakov, V. N.; Smetannikov, Yu., V. Vysokomol Soed, Ser A 1996, 38(9), 1467–1471.
[5] Tarasova, N. P.; Smetannikov, Yu., V.; Kochetov, I. N.; Mikhaylova, E. G. Izv Vuz Chem Chem Technol 1998, 41(1), 117–120.
[6] Tarasova, N. P.; Smetannikov, Yu., V.; Mikhaylov, E. G Dokl Akad Nauk 1998, 360(1), 69–72.
[7] Tarasova, N. P.; Smetannikov, Yu., V.; Polyiansky, D. E. Green Industrial Applications of Ionic Liquids; Rodgers, R. D., et al. (Eds.); Kluwer Academic Publishers: Boston, MA, 2003; pp. 537–544.
[8] Astakhova, G. V., Korolev, V. V.; Kamorskiy, S. V. Ser. mineral fertilizers and sulfuric acid. Survey information; NIITEKHIM, M., 1987, 46.
[9] Katayama, Y.; Mizutani, T.; Utsumi, W.; Shimomura, O.; Yamakata, M.; Funakoshi, K. Nature 2000, 403, 170–173.
[10] Ballone, P.; Jones, R. O. J Chem Phys 2004, 121(16), 8147–8157.
[11] Hohl, D.; Jones, R. O. Phys Rev B 1994, 50(23), 17047–17053.
[12] Hasegawa, A.; Wyatt, J. L.; Symons, M. C. R. J Chem Soc, Chem Commun 1990, 62.
[13] Scheer, M.; Dargatz, M.; Schenzel, K.; Jones, P. G. J Organomet Chem 1992, 435(1–2), 123–132.
[14] Jones, R. O.; Ganteför, G.; Hunsicker, S.; Pieperhoff, P. J Chem Phys 1995, 103, 9549.
[15] Guo, L.; Wu, H.; Jin, Zh. J Mol Struct THEOCHEM 2004, 59, 677.
[16] Tarasova, N. P.; Artemkina, I. M.; Smetannikov Yu. V. In XIV Conference on the Chemistry of Phosphorus Compounds, Kazan, Russia, 27 June–1 July 2005; Abstracts, P132.
[17] Jones, R. O.; Hohl, D. J. J Chem Phys 1990, 92, 6710.
[18] Brundle, C. R.; Kuebler, N. A.; Robin, M. B.; Basch, H. Inorg Chem 1972, 11, 20.
[19] Huang, R.; Li, H.; Yang, Sh. J Phys Chem 1995, 99, 1418.
[20] Pauling, L.; Simonetta, M. J Chem Phys 1952, 20, 29.
[21] Moffitt, W. E. Trans Faraday Soc 1948, 44, 987.
[22] Ballone, P.; Jones, R. O. J Chem Phys 1994, 100(7), 4941–4946.
[23] Bader, R. F. W. Atoms in Molecules. A Quantum Theory; Clarendon Press: Oxford, UK, 1990.
[24] Tsirelson, V. G.; Ozerov, R. P. Electron Density and Bonding in Crystals; Institute of Physics Publishing:, Bristol, UK, 1996.
[25] Tsirelson, V. G. Chemical Bond and Thermal Agitation of Atoms in the Crystals; VINITI: Moscow, 1993.
[26] Hernandez-Trujillo, J.; Bader, R. F. W. J Phys Chem A 2000, 104(8), 1779.
[27] Popelier, P. L. A. Coord Chem Rev 2000, 197, 169.
[28] All quantities in this work are given in the atomic units, except the bond distances, which are given in angstrom.
[29] Marabello, D.; Bianchi, R.; Gervasio, G.; Cargnoni, F. Acta Crystallogr, Sect A: Found Crystallogr 2004, 60, 494.
[30] Granovsky A. A. GAMES; available at http://classic.chem.msu.su/gran/gamess/index.html.
[31] Schmidt, M. W.; Baldridge, K. K.; Boatz, J. A.; Elbert, S. T.; Gordon, M. S.; Jensen, J. J.; Koseki, S.; Matsunaga, N.; Nguyen, K. A.; Su, S.; Windus, T. L.; Dupuis, M.; Montgomery, J. A. J Comput Chem 1993, 14, 1347.